

Giant electrostrictive effects of $\text{NaNbO}_3\text{-BaTiO}_3$ lead-free relaxor ferroelectrics

Ruzhong Zuo,^{1,a)} He Qi,¹ Jian Fu,¹ Jingfeng Li,² Min Shi,¹ and Yudong Xu¹

¹Institute of Electro Ceramics and Devices, School of Materials Science and Engineering, Hefei University of Technology, Hefei 230009, People's Republic of China

²State Key Laboratory of New Ceramics and Fine Processing, Department of Materials Science and Engineering, Tsinghua University, Beijing 100084, People's Republic of China

(Received 15 April 2016; accepted 21 May 2016; published online 7 June 2016)

A giant electrostrictive effect was observed in $(1-x)\text{NaNbO}_3\text{-xBaTiO}_3$ relaxor ferroelectric ceramics, which exhibit a high electrostrictive coefficient Q_{33} of $\sim 0.046 \text{ m}^4/\text{C}^2$ twice as large as those of Pb- and Bi-based perovskite relaxor ferroelectric ceramics. The theoretical analysis suggests that Q_{33} should be strongly correlated with chemical species of cations in a perovskite structure in which a strong ionic bond is of great benefit compared with a covalent bond. A hysteresis-free large electrostrictive strain of $\sim 0.148\%$ up to at least 70 Hz was obtained in the $x = 0.25$ sample, demonstrating significant advantages over piezoelectric effects in high-precision ceramic actuators. *Published by AIP Publishing.* [<http://dx.doi.org/10.1063/1.4953457>]

Piezoelectric ceramics have been widely applied in ceramic actuators owing to their excellent electromechanical properties, particularly $\text{Pb}(\text{Zr,Ti})\text{O}_3$ (PZ-PT)-based solid solutions. However, strain hysteresis ($\sim 10\%$ – 20%) from reversible non- 180° domain switching has restricted their applications requiring high positioning precision. Compared with piezoelectric effects, the electrostrictive effect offers several unique advantages such as little or no strain hysteresis up to high frequencies, a fast response speed, reduced aging effects, and no poling requirement.^{1,2} It is a fundamental property for a dielectric which changes its dimensions under an applied bias electric field. The electric field induced longitudinal strain (S_{33}) can be expressed by a quadratic function of the polarization (P_3), $S_{33} = Q_{33}P_3^2$, where Q_{33} is the electrostrictive coefficient. In normal perovskite ferroelectrics, the strain does not obey a linear relationship with P^2 because of the existence of some other contributions such as converse piezoelectric effect and domain switching.³ Generally, the electrostrictive effect is very weak in most perovskites, and the electrostrictive strain is usually small compared with that from the converse piezoelectric effect.

A large hysteresis-free electrostrictive strain up to $\sim 0.1\%$ has been reported in some lead-based relaxor ferroelectrics with a large Q_{33} value of $\sim 0.02 \text{ m}^4/\text{C}^2$,¹⁻⁴ among which $\text{Pb}(\text{Mg}_{1/3}\text{Nb}_{2/3})\text{O}_3$ (PMN) is a typical one. However, the use of the lead would cause the environment pollution owing to its toxicity. A lot of work has been done in recent years on the development of lead-free electrostrictive materials such as $(\text{Bi}_{0.5}\text{Na}_{0.5})\text{TiO}_3$ (BNT)^{-5,6} and BaTiO_3 (BT)^{-7,8} based materials, in which a large Q_{33} value was also reported. However, for these nonlinear dielectrics, achievable strains are limited by either their insufficient Q_{33} values or not high enough saturated polarization associated with dielectric permittivity ($dP = \epsilon \cdot dE$). Therefore, it would be of much interest to explore larger- Q_{33} electrostrictive materials

for their actuator applications. Although it is known that Q_{33} increases with increasing the ordering degree of B-site cations in perovskite ferroelectrics,¹ further investigation is still required to disclose the origin of high Q_{33} values.

In this study, a highly pure hysteresis-free electrostrictive strain was reported in $(1-x)\text{NaNbO}_3\text{-xBaTiO}_3$ ($(1-x)\text{NN-xBT}$) solid-solution ceramics, which was ascribed to both giant Q_{33} values and relatively large dielectric permittivity. Furthermore, origin of high Q_{33} values was explored by means of the analysis of Born effective charges \bar{Z}_{33}^* as an estimation of the contribution of cations to the polarizability.⁹ No work has been done so far from this point of view.

The $(1-x)\text{NN-xBT}$ ceramics ($x = 0.15\text{--}0.25$) were prepared by a conventional solid-state process using high-purity raw materials of Na_2CO_3 , Nb_2O_5 , BaCO_3 , and TiO_2 . The powders in stoichiometric proportions were mixed thoroughly in ethanol using zirconia balls for 12 h. The mixture was ball-milled again for 24 h after calcination at 900°C for 5 h. The as-pressed samples were sintered at $1240\text{--}1300^\circ\text{C}$ for 2 h in air. Silver electrodes were fired on both sides of the disk samples at 550°C for 30 min.

Dielectric properties as a function of temperature and frequency were measured by an LCR meter (Agilent E4980A, Santa Clara, CA). The ferroelectric testing system (Precision Multiferroic, Radiant Technologies, Inc., Albuquerque, NM) connected with a laser interferometric vibrometer (SP-S 120, SIOS Meßtechnik GmbH, Germany) were used to measure polarization versus electric field (P-E) hysteresis loops and strain versus electric field (S-E) curves.

The dielectric property of $(1-x)\text{NN-xBT}$ ceramics was measured as a function of temperature and frequency, as shown in Fig. 1(a). It can be found that the dielectric maxima at the phase transition temperature (T_m) slightly decreased with increasing x . However, the dielectric peak at T_m was found to be broader and more frequency-dependent, as reflected by the variation of the diffuseness degree (γ) and another parameter $\Delta T_{\text{relax}} = T_{m, 1 \text{ MHz}} - T_{m, 1 \text{ kHz}}$ (see the inset of Fig. 1(a)). Accordingly, the T_m value dropped from

^{a)}Author to whom correspondence should be addressed. Electronic addresses: piezolab@hfut.edu.cn and rzzuo@hotmail.com. Tel.: 86-551-62905285. Fax: 0086-551-62905285.

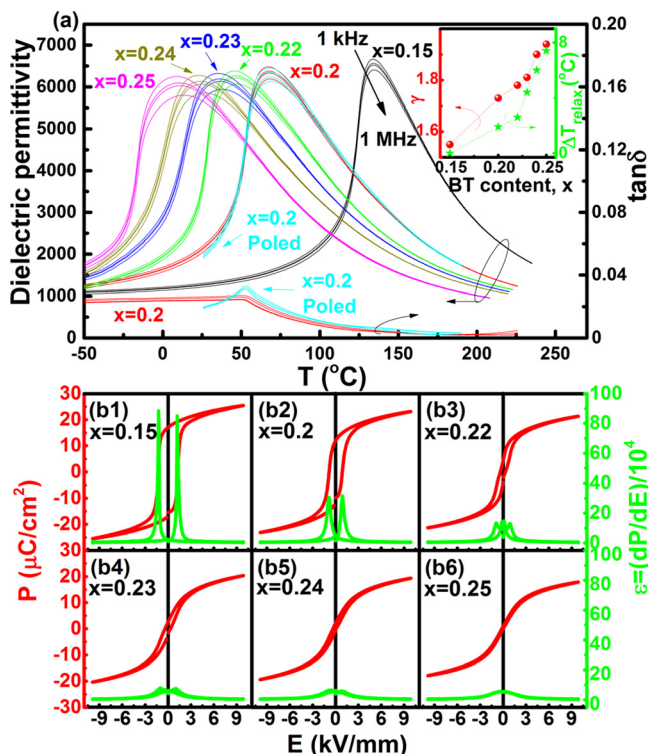


FIG. 1. (a) Temperature and frequency dependent dielectric properties of unpoled $(1-x)$ NN- x BT ceramics in compared with those of poled $x=0.2$ sample; the inset in (a) shows the variation of two parameters γ and ΔT_{relax} with changing x , and (b) polarization and dielectric response dP/dE during electric cycling measured at room temperature at 10 Hz for the ceramics with (b1) $x=0.15$, (b2) $x=0.2$, (b3) $x=0.22$, (b4) $x=0.23$, (b5) $x=0.24$ and (b6) $x=0.25$.

$\sim 130^\circ\text{C}$ for the $x=0.15$ sample to below room temperature for samples with $x \geq 0.24$. This illustrated that the addition of BT tended to disrupt long-range ordered ferroelectric state of NN-BT into polar nanoregions (PNRs), which are typical features of relaxor ferroelectrics. Accompanied by the enhancement of relaxation degree, the $(1-x)$ NN- x BT samples would undergo a transition from nonergodic states to ergodic states at room temperature as a result of increased local random fields. By comparing dielectric properties of the $x=0.2$ sample before and after poling, it can be found that this composition belonged to a nonergodic state at room temperature but should be located close to the critical temperature from nonergodic to ergodic states because the loss peak near room temperature became sharper after poling.

Figure 1(b) demonstrates P-E loops and corresponding dielectric response ($\epsilon = dP/dE$) for $(1-x)$ NN- x BT ceramics. The $x=0.15$ and $x=0.2$ samples showed a square P-E loop, which conforms to the feature of a weak relaxor ferroelectric with a nonergodic state at room temperature. A sharp dielectric peak as a result of rapid domain reorientation could be found near the coercive field (E_c), suggesting a large polarization hysteresis between $-E_c$ and E_c . On the one hand, the polarization hysteresis was found to decrease with increasing electric field, such that a hysteresis-free polarization part could be found approximately at $E > 2E_c$. On the other hand, the remanent polarization (P_r) started to decrease sharply at $x=0.22$. A slim P-E loop with a very small P_r was found for compositions with $x \geq 0.22$. Particularly, a pinched P-E loop together with a double-peak dielectric response could be seen

in the composition of $x=0.22$, which was usually correlated with the coexistence of nonergodic and ergodic states.^{10,11} At higher BT contents, the polarization hysteresis and the dielectric peak were found to be significantly reduced owing to the weakening of ferroelectricity. A hysteresis-free P-E loop was generated in the composition of $x=0.25$. This might be related to the enhanced dynamics and reduced size of PNRs caused by the substitution of BT. For the same reason, it can be deduced that the $x > 0.22$ sample should belong to the ergodic relaxor state at room temperature.

The corresponding S-E bipolar strain curves of $(1-x)$ NN- x BT ceramics are shown in Fig. 2(a). It can be seen that S-E curves gradually changed from a butterfly shape to a sprout shape with increasing x , accompanied by an obvious decrease of the negative strain (S_{neg}). S_{neg} has become zero since $x > 0.22$, indicating $x > 0.22$ samples have entered the ergodic phase zone at room temperature. This keeps a good agreement with the dielectric measurement (Fig. 1(a)). Simultaneously, the hysteresis of S-E curves decreased, and disappeared completely at $x=0.25$. A slight hysteresis of strains for samples with $x=0.22-0.24$ should be ascribed to the time effect of back-switching of electric field induced ergodic to ferroelectric phase transition.^{12,13} Figs. 2(b)-2(d) show the strain versus polarization (S-P) curves for three representative samples ($x=0.15$, $x=0.22$, and $x=0.25$), which are located at nonergodic phase zone, the ergodic-nonergodic mixed phase zone, and pure ergodic phase zone, respectively. The serious hysteresis has made the S-P curve deviate from a quadratic relationship for the $x=0.15$ sample, compared with the $x=0.22$ and $x=0.25$ samples. If one compared Fig. 2(b) with Fig. 2(a), it seems that this deviation in S-P curves was mainly caused by the negative strain induced by irreversible domain switching. Moreover, the $x=0.25$ sample exhibited a hysteresis-free electrostrictive strain of as large as 0.148% and a typical characteristic of nonlinear dielectrics that the polarization saturation at higher fields deviates from a linear relationship (Fig. 1(b6)) and the electrostrictive strain is a quadratic function of polarization instead of electric field

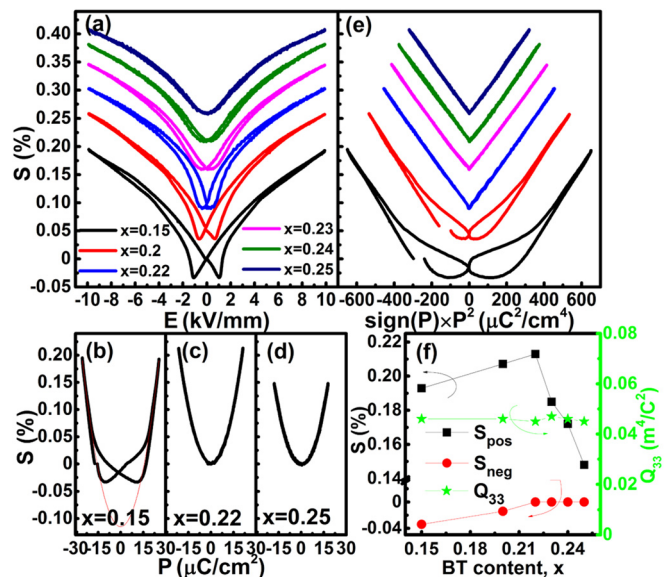


FIG. 2. (a) S-E, (b)-(d) S-P curves and (e) S-P² curves for $(1-x)$ NN- x BT ceramics as indicated, and (f) the variation of Q_{33} , S_{pos} and S_{neg} with x .

(Figs. 2(a) and 2(d)). For the same reason, S-P² relations are pretty linear for samples with $x \geq 0.22$, but only at higher fields for samples with $x < 0.22$ (Fig. 2(e)). Under a strong electric field, the domains could be clamped and the influence of domain switching would be eliminated, such that the linear increase of polarization merely originated from the ionic displacement. The Q_{33} value of $(1-x)\text{NN-xBT}$ ceramics with respect to composition could be obtained by linearly fitting S-P² curves, as plotted in Fig. 2(f). The variation of Q_{33} with composition was quite small as compared with their dielectric and ferroelectric properties.^{4,5} It is on the order of 0.045–0.048 m⁴/C² for all studied compositions although these samples underwent a nonergodic to ergodic phase transition. Moreover, it can be seen from Fig. 2(f) that both positive strains (S_{pos}) and S_{neg} dramatically varied with x . S_{pos} reached the maximum ($\sim 0.22\%$) at $x = 0.22$ as S_{neg} dropped to zero, further indicating that the $x = 0.22$ sample was located at the boundary of nonergodic and ergodic phases. The $x = 0.25$ sample owned a pure ergodic state at room temperature, as can be also seen from its dielectric-temperature curves (Fig. 1(a)) and P(S)-E curves (Figs. 1(b) and 2(a)).

Interestingly, the nonlinear part on the S-P² curves started to disappear in ergodic relaxors, suggesting that strains of these compositions ($x > 0.2$) are dominated by an electrostrictive effect. To achieve a hysteresis-free electrostrictive strain, macroscopic domain reorientation should be avoided. The ergodic relaxors should show an isotropic cubic structure on the macroscopic scale at zero fields. The orientation and growth of PNRs as a result of a strong electric field would make the polarization response deviate from the linear relation with electric field. However, the rapid disruption of field induced long-range ferroelectric ordering on the ergodic matrix would generate a hysteresis-free strain response to electric field as external field was released. This is practically true in the $x = 0.25$ sample since it owns a strong ergodicity or a large enough local random field. By comparison, an obvious strain hysteresis of $\sim 20\%$ could be seen on the S-E curve of the $x = 0.22$ ceramic, which is on the same level as that in normal piezoelectric ceramics (10%–20%).^{14,15}

The strain response of $(1-x)\text{NN-xBT}$ ceramics was also explored as a function of temperature. The S-P² curves under different measuring temperatures are shown in Figs. 3(a)–3(c) using the $x = 0.15$, $x = 0.22$, and $x = 0.25$ compositions as examples. It can be found that the nonlinear part in S-P² curves of the $x = 0.15$ sample gradually disappeared with increasing temperature because the sample underwent a transition from nonergodicity to ergodicity. A linear relation of S against P² for the $x = 0.22$ and $x = 0.25$ samples could be seen in the whole measuring temperature range, indicating these two samples have been dominated by ergodic phases at room temperature. According to the slope of the linear part of S-P² curves, Q_{33} was calculated as a function of temperature for different samples, as shown in Fig. 3(d). It is quite stable (0.0445–0.0465 m⁴/C²) in a wide temperature range, suggesting that Q_{33} in $(1-x)\text{NN-xBT}$ is also insensitive to temperature. On the contrary, the dielectric and ferroelectric properties generally are usually both composition and temperature dependent. It is worthy of note that Q_{33} of $(1-x)\text{NN-xBT}$ is much larger than that of PMN- (~ 0.025 m⁴/C²),^{1–3} PZT- (~ 0.021 m⁴/C²),^{4,16} and BNT- (~ 0.025 m⁴/C²)^{5,6} based

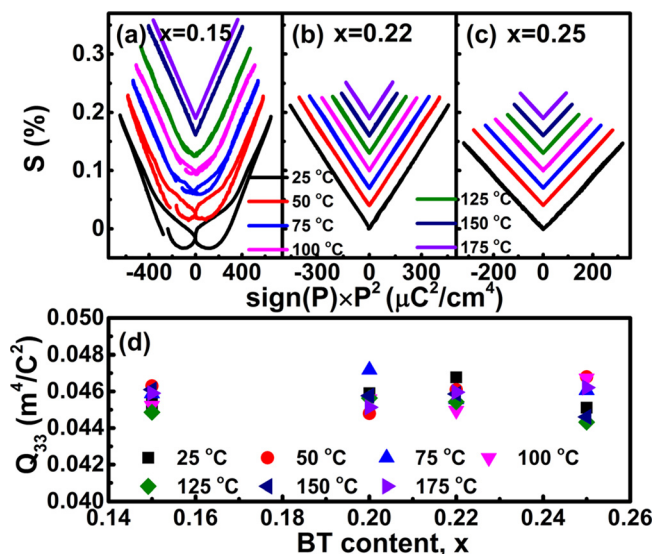


FIG. 3. S-P² curves measured at various temperatures for the ceramics with (a) $x = 0.15$, (b) $x = 0.22$ and (c) $x = 0.25$, and (d) the variation of Q_{33} with changing x , as determined by linearly fitting S-P² curves.

ceramics, and slightly higher than that of BT-based ceramics (0.040–0.045 m⁴/C²).^{7,8} Of special interest is that the $x = 0.25$ sample might also own a hysteresis-free large electrostrictive strain of $\sim 0.148\%$, which is probably attributed to its relatively high dielectric permittivity (~ 6000 at 1 kHz at 25 °C) in addition to its high Q_{33} (its small-field electrostrictive coefficient $M_{33} = Q_{33} \cdot \epsilon_{33}^2 \sim 1.3 \times 10^{-16}$ m²/V²). The $x = 0.24$ sample might have a slightly higher electrostrictive strain ($\sim 0.172\%$) than the $x = 0.25$ sample probably because it has a relatively high dielectric permittivity (ca. 6300 at 1 kHz at 25 °C, see Fig. 1). However, its strain hysteresis is larger as a result of the difference in dynamics of PNRs (T_m at 1 kHz at $x = 0.24$ is ~ 22.3 °C, but ~ 9 °C at $x = 0.25$, see Fig. 1(a)), as can be seen from the S-E curve in Fig. 2(a).

Figure 4 shows the frequency dependence of unipolar strains for the $x = 0.15$ and $x = 0.25$ samples, which belong to nonergodic phases and ergodic phases at room temperature, respectively. It can be seen that the strain hysteresis slightly increased with increasing frequency for the $x = 0.15$ sample. By comparison, the $x = 0.25$ sample exhibited a hysteresis-free unipolar strain in a wide frequency of 0.1 Hz up to 70 Hz. Compared with the $x = 0.25$ sample, the $x = 0.15$ sample has a large strain hysteresis which is also frequency dependent to some extent. This strain hysteresis should be ascribed to the existence of reversible non-180° domain switching during the period of applying electric fields. When the measuring frequency increases, the domain wall motion lags and then its contribution to the strain level also drops, as clearly shown in the inset of Fig. 4(b). The $x = 0.25$ composition is an ergodic relaxor at room temperature, where the PNRs exist in a dynamic state with small size and meanwhile the thickness of domain walls (the regions where polarization is not well-defined) is comparable with the size of nanodomains.¹⁷ Thus, both PNRs and domain walls would exhibit a fast response to the applied field, leading to a hysteresis-free unipolar strain and frequency-insensitive strain magnitude for the $x = 0.25$ sample. Of course, the difference of the size of PNRs would also induce

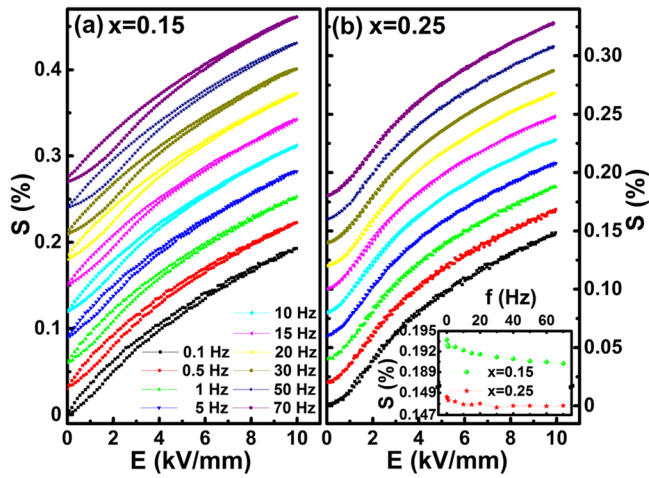


FIG. 4. The unipolar S-E curves measured at different frequencies for the ceramic samples with (a) $x=0.15$ and (b) $x=0.25$; the inset shows the strain magnitude against logarithmic frequency of these two samples as indicated.

a little hysteresis even for ergodic compositions in some cases, as can be seen in the $x=0.22$ – 0.24 compositions from Fig. 2(a). Hysteresis-free large electrostrain ($\sim 0.148\%$) up to at least 70 Hz in the $x=0.25$ sample would offer significant advantages in high-precision ceramic actuators, compared with piezoelectric effects.

It is known that electrostriction originates from the cations shifting away from their natural equilibrium positions.¹⁸ In centrosymmetric ABO_3 perovskite crystals, the equilibrium positions should be the center of O_{12} and O_6 polyhedrons for A-site and B-site cations, respectively. The contribution of the cations to the polarizability can be estimated by the average Born effective charge \bar{Z}_{33}^* .^{9,19} With applying a certain bias electric field E_3 , the average S_{33} and P_3 for per unit volume can be calculated using a Boltzmann distribution as follows:

$$S_{33} = (3gq^2/4f^3r_0) \cdot E_3^2, \quad (1)$$

$$P(A/B) = \bar{Z}_{33}^*(A/B) \cdot D(A/B), \quad (2)$$

where r_0 denotes the equilibrium position, q is the charge of cations and D is the off-center displacement from the corresponding O cage. The coefficients g and f are associated with the crystal structure and the features of the cations. Thus, when ignoring the difference of both lattice parameters and the order degree between different systems, Q_{33} of each unit cell seems to be strongly correlated with $\Sigma q^2/\bar{Z}_{33}^{*2}$. The Q_{33} values for a few typical perovskite systems were plotted against $\Sigma q^2/\bar{Z}_{33}^{*2}$, as shown in Fig. 5. It can be found that Q_{33} generally tended to increase proportionally with increasing the value of $\Sigma q^2/\bar{Z}_{33}^{*2}$. The relatively high $\Sigma q^2/\bar{Z}_{33}^{*2}$ values in NN-based ceramics show advantages in electrostrictive effect over conventional Pb-based and Bi-based perovskite systems. By comparison, the relatively low dielectric permittivity might counteract the contribution of large Q_{33} values to strains for SrTiO_3 (ST) and KTaO_3 (KT) quantum paraelectrics.²⁰ It is generally believed that \bar{Z}_{33}^* should be correlated with chemical species of the cations. Compared with

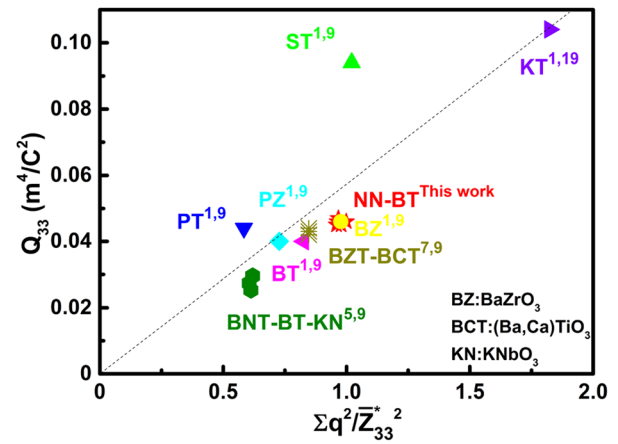


FIG. 5. Schematic relationship of Q_{33} and $\Sigma q^2/\bar{Z}_{33}^{*2}$ for a few typical perovskite dielectric ceramics.

strongly covalent cations, the values of \bar{Z}_{33}^* are close to their nominal ionic charges for cations with strong ionic behavior. A strong dynamic charge transfer would take place along the O-cation bond as the bond length is varied for a covalent bond, thus leading to a large \bar{Z}_{33}^* value. It would then become weak with enhancing the ionic character of the O-cation bond. As a result, the cation with a stronger ionic bond with oxygen shows larger $\Sigma q^2/\bar{Z}_{33}^{*2}$. Moreover, most of perovskite ferroelectrics usually have similar weakly ionic O-B bonds. However, there is a big difference between A-site cations, for example, Pb and Bi should exhibit a strong covalency with oxygen owing to the hybridization of 6s orbitals with O 2p orbitals while Na, K, Ba, etc., should show a strong ionic behavior. For NN-based relaxor ferroelectrics, a large electrostrictive strain would be generated owing to high Q_{33} from a strong A-O ionic bond and simultaneously high polarization response (P_3) from B-site ionic ferroelectric displacement.

In summary, the electrostrictive effect in $(1-x)\text{NN}-x\text{BT}$ lead-free relaxor ferroelectric ceramics was investigated as a function of composition, temperature, and frequency. With the increase of the relaxor degree, a pure hysteresis-free large electrostrictive strain of $\sim 0.148\%$ was obtained in the $x=0.25$ sample. It was attributed to not only high dielectric permittivity (~ 6000 at 1 kHz) but also high electrostrictive coefficient Q_{33} ($\sim 0.046 \text{ m}^4/\text{C}^2$) which is almost twice those of Pb-based and Bi-based perovskite relaxor ceramics. This large Q_{33} was found to be insensitive to the variation of both composition and temperature. Theoretical analysis indicated that Q_{33} should be strongly correlated with chemical species of cations in a perovskite structure in which a strong ionic bond is of great benefit compared with a covalent bond. Such a large hysteresis-free electrostrictive strain up to at least 70 Hz would offer significant advantages over piezoelectric effects in high-precision ceramic actuators.

Financial support from the National Natural Science Foundation of China (Grant Nos. 51472069, U1432113, 51402079, and 51332002) and the Anhui Provincial Natural Science Foundation (1508085JGD04) is gratefully acknowledged.

- ¹K. Uchino, S. Nomura, L. E. Cross, R. E. Newnham, and S. J. Jang, *J. Mater. Sci.* **16**, 569 (1981).
- ²J. Coutte, B. Dubus, J. C. Debus, C. Granger, and D. Jones, *Ultrasonics* **40**, 883 (2002).
- ³F. Li, L. Jin, Z. Xu, D. W. Wang, and S. J. Zhang, *Appl. Phys. Lett.* **102**, 152910 (2013).
- ⁴G. H. Haertling, *Ferroelectrics* **75**, 25 (1987).
- ⁵J. Li, F. Wang, X. Qin, M. Xu, and W. Shi, *Appl. Phys. A* **104**, 117 (2011).
- ⁶S. T. Zhang, A. B. Kounga, W. Jo, C. Jamin, K. Seifert, T. Granzow, J. Rödel, and D. Damjanovic, *Adv. Mater.* **21**, 4716 (2009).
- ⁷F. Li, L. Jin, and R. P. Guo, *Appl. Phys. Lett.* **105**, 232903 (2014).
- ⁸S. Y. Zheng, E. Odendo, L. J. Liu, D. P. Shi, Y. M. Huang, L. L. Fan, J. Chen, L. Fang, and B. Elouadi, *J. Appl. Phys.* **113**, 094102 (2013).
- ⁹W. Zhong, R. D. King-Smith, and D. Vanderbilt, *Phys. Rev. Lett.* **72**, 3618 (1994).
- ¹⁰R. Z. Zuo, F. Li, J. Fu, D. G. Zheng, W. L. Zhao, and H. Qi, *J. Eur. Ceram. Soc.* **36**, 515 (2016).
- ¹¹Y. Ehara, N. Novak, S. Yasui, M. Itoh, and K. G. Webber, *Appl. Phys. Lett.* **107**, 262903 (2015).
- ¹²J. Shi, H. Q. Fan, X. Liu, and Q. Li, *J. Eur. Ceram. Soc.* **34**, 3675 (2014).
- ¹³W. L. Zhao, R. Z. Zuo, J. Fu, and M. Shi, *J. Eur. Ceram. Soc.* **34**, 2299 (2014).
- ¹⁴H. Kungl, T. Fett, S. Wagner, and M. J. Hoffmann, *J. Appl. Phys.* **101**, 044101 (2007).
- ¹⁵D. W. Wang, M. S. Cao, and S. J. Zhang, *J. Am. Ceram. Soc.* **95**, 3220 (2012).
- ¹⁶P. M. Weaver, M. G. Cain, and M. Stewart, *Appl. Phys. Lett.* **96**, 142905 (2010).
- ¹⁷D. S. Fu, H. Taniguchi, M. Itoh, S. Y. Koshihara, N. Yamamoto, and S. Mori, *Phys. Rev. Lett.* **103**, 207601 (2009).
- ¹⁸K. Uchino, S. Nomura, K. Vedam, R. E. Newnham, and L. E. Cross, *Phys. Rev. B* **29**, 6921 (1984).
- ¹⁹S. Cabuk, *Phys. Status Solidi B* **247**, 93 (2010).
- ²⁰G. A. Samara, *J. Phys.: Condens. Matter* **15**, R367 (2003).